arXiv:cond-mat/0408188v3 [cond-mat.other] 11 Sep 2004

Resonant two-photon excitation of 1s paraexcitons in Cuprous Oxide

Yingmei Liu, David Snoke

Department of Physics and Astronomy

University of Pittsburgh, Pittsburgh, PA 15260

(Dated:)

Abstract

We have created paraexcitons in Cu_2O via resonant two-photon generation, and examined their population dynamics by means of time-correlated single photon detection. Confining the excitons to a constant volume in a harmonic-potential trap made with inhomogeneous applied stress along the [001] axis, we find that paraexcitons are created directly, and orthoexcitons appear primarily through a up-conversion of the paraexcitons. Hot excitons are also created via a three-photon process when the IR laser is non-resonant. Also we generate excitons with two colliding pulses, and the luminescence is weaker than that from one beam excitation with same total laser power. These results show that resonant one-beam two-photon generation of paraexcitons is a promising way to pursue Bose-Einstein condensation of paraexcitons.

PACS numbers:

I. INTRODUCTION

Naturally-grown high-quality Cu_2O is a good candidate for studying excitonic Bose-Einstein condensation. First, an inversion symmetry in Cu_2O forbids any direct dipole recombination of excitons, which gives the exciton a long lifetime up to microseconds. Second, Cu_2O is a direct-gap semiconductor with repulsive exciton-exciton interactions, which means the electron-hole liquid (EHL) is not stable[1]. Moreover, the large binding energy of the excitons (150 meV) is equivalent to a temperature of 1740 Kelvin, which allows excitons to exist at room temperature[2]. The lowest excitonic state is the 1s-"yellow" exciton series, consisting of electrons in the Γ_6^+ level of the conduction band and holes in the Γ_7^+ level of the valence band with 2.173 eV gap energy. By electron-hole exchange, the "yellow" excitons split into a triplet orthoexciton and a singlet paraexciton, which lies 12 meV lower[2].

Most studies[2,3,4] have concentrated on the higher-lying orthoexciton state since it can be easily created by a single-photon phonon-assisted absorption. In the single-photon phonon-assisted excitation process, however, a hot optical phonon is created which can heat the exciton gas, thereby deterring BEC. In the past few years, several groups[5,6,7,8,9,10,11,12] have tried resonant two-photon excitation of the orthoexciton state. A major advantage is that the scattered two-photon laser light will not damage imaging systems because it is far away from the exciton luminescence lines, which allows a measurement during the laser pulse. It is also expected that two colliding pulses in opposite directions will create excitons directly in the $\vec{k} = 0$ state, where a condensate should appear, instead of in a state with finite momentum.

Resonant excitation of orthoexcitons still has the problem that the orthoexcitons will convert down into paraexcitons by a phonon emission[1], and the emitted phonon will cause a local heating, which may prevent BEC. Our present work aims to solve the above problem with a resonant two-photon excitation of the yellow paraexciton state, because it is the lowest exciton state and primarily only decays by direct single-photon emission. We create excitons in a harmonic potential trap made with an external stressor[2,4,13], which confines excitons in a defined volume and changes the local symmetry of Cu_2O from O_h to D_{4h}. One problem which becomes more important in the potential trap is the Auger recombination process, which happens when two excitons collide and one exciton ionizes, taking the energy of the other exciton that recombined. Therefore the Auger process not only gives a severe limit

in exciton density but also heats up the exciton gas, which will tend to prevent BEC. The Auger recombination rate increases roughly as the square of the stress, with much smaller Auger recombination at the stress lower than 1.5 kbar[2,14]. However, because the phonon-assisted orthoexciton and direct paraexciton luminescence lines are separated at high stress but substantially overlapped at low stress[13], we have to use high stress to separate the luminescence lines. In this work, the inhomogeneous applied stress is kept at 1.9 kbar, a trade-off point which is good enough to spectrally separate the paraexciton line and provides a relatively small Auger process.

In this paper, we present experimental results for two experimental configurations, with one IR laser beam and with two colliding IR laser pulses. We demonstrate the resonant creation of paraexcitons under two-photon excitations with several strong evidences. Then we propose a model of the excitation mechanism for the paraexciton and orthoexciton in the two-photon excitations, based on our study on selection rules and polarization dependence of the yellow excitons from group theory.

II. EXPERIMENTAL SET-UP

The Cu_2O sample, a $4.9\times3\times3$ mm bulk crystal, is immersed in the liquid helium in a Janis optical cryostat, at a temperature controlled by a homemade PID temperature controller. The lowest temperature in the cryostat is 1.6 Kelvin. As shown in Fig. 1, in one-beam experiments the sample is oriented as follows: one [110] surface is illuminated by an IR laser beam and the exciton luminescence is collected from the perpendicular $[\bar{1}10]$ surface by an imaging lens which focuses the light onto the entrance slit of a $\frac{1}{4}$-meter spectrometer, with a choice of a CCD camera and a photo-multiplier tube (PMT) as detectors. The exciton population dynamics are examined by means of time-correlated single photon detection. We can also create excitons by splitting the IR laser beam into two counter-propagating parts which meet in the Cu_2O sample at the same time from opposite [110] directions, with a controlled time delay. The repetition rate, the duration and the spectral width of the IR laser are 250 KHz, 200 fs and 20 nm, respectively. In order to compare, we also do experiments under single-photon excitation with a cavity-dumped 3.8 MHz and 50 ps red dye-laser tuned to the exciton resonance for the same crystal orientation.

Excitons are confined by a harmonic potential trap made with a 6 mm radius curved glass

stressor applied along the [001] axis from the top surface of the Cu_2O crystal. Under the [001] stress, we find strong paraexciton signal, although Naka and Nagasawa[5] reported that paraexcitons were too weak to be detected. The main reason is that our femto-second laser system has much greater instantaneous intensity than their nano-second laser. Moreover, the exciton luminescence is collected from a direction perpendicular to the incident laser beam in this work, which has several advantages over their forward scattering geometry[5,11,12]. For example, the second harmonic scattering of the incident infrared laser light does not mix with the exciton luminescence.

III. ONE-BEAM, TWO-PHOTON EXCITATION

A. Two-photon or three-photon process?

When we create excitons with an IR laser, the first question which arises is how we can say it is not a three-photon or four-photon excitation, but a two-photon excitation. One way to answer this question is from the dependence of the exciton luminescence intensity on the IR laser power, that is to say, the excitation is a n-photon process if the intensity of exciton luminescence is proportional to (laser-power)^n. We performed a series of experiments for a broad wavelength range of IR lasers, with an inhomogeneous stress of 1.9 kbar along the [001] direction and the paraexciton line position at 614.1 nm. As shown in Fig. 2, our experimental results indicate that the excitation is a two-photon process when the IR laser is at the paraexciton resonant position, and it is a three-photon process under off-resonant IR laser, for example at 1240 nm. All experiments in the following discussions are under resonant two-photon excitation of the paraexciton state. We note that even at this wavelength, the three-photon process will be responsible for about 25% of the total exciton creation at the highest laser powers we use, and it will dominate at high excitation power, which may also create another barrier to BEC.

B. Strong evidence for resonant paraexciton excitations

With an IR laser tuned to one half the paraexciton ground-state energy, several experimental results convince us that we directly create paraexcitons, and orthoexcitons primarily come from the excitonic Auger process. The first strong evidence is shown in Fig. 3, the

time-integrated luminescence intensity as a function of IR laser power from 55 mW to 3 mW. As mentioned above, under the 1.9 kbar stress along the [001] direction, the direct paraexciton line is at 614.1 nm. Although paraexcitons primarily only decay by single-photon emission, there are two emission lines for orthoexcitons, as shown in Fig. 3, the direct orthoexciton luminescence line at 611.7 nm, which corresponds to emission of a single photon, and phonon-assisted orthoexciton luminescence line at 615.7 nm, which corresponds to emission of a single photon and a Γ_{12}^{-} optical phonon with energy of 13.8 meV. There is only paraexciton luminescence when the laser power is very low, indicating that the resonant IR laser creates the paraexciton directly. Orthoexcitons start to appear at higher laser power, around 5 mW as seen in Fig. 3, and become stronger and stronger relative to the paraexcitons with increasing the laser power, which implies that orthoexcitons are created not directly by the laser, but by a density-dependent process from paraexcitons.

A second evidence is found in time-resolved paraexciton luminescence data. Fig. 4 shows paraexciton luminescence intensity as a function of time after laser pulses in two different pulse-laser excitations. In one case, two-photon excitation resonant with the paraexciton state is used, and in the second case, single-photon excitation tuned to the bottom of the orthoexciton phonon-assisted absorption is used. The average powers of the IR laser and the red laser used in the excitations were adjusted to get the same total integrated exciton luminescence intensity. These average powers were 70 mW and 0.9 mW, respectively. There are several similarities between the two cases. The paraexciton luminescence intensity in both cases reaches a steady-state value long after the laser pulses which indicates lifetimes of paraexcitons longer than the 260 ns period between the laser pulses, and the paraexciton luminescence intensities at time just before the laser pulses are comparable, equal to the steady-state value left from the previous laser pulse. However, in the case of resonant two-photon excitation, the paraexcitons reach maximum intensity immediately after the laser pulse, consistent with the paraexcitons being created directly by the laser. In the case of single-photon excitation of orthoexcitons, paraexcitons do not appear right after the laser pulse, but are slowly created in a time interval of more than 10 ns from a process which is known to be phonon-assisted orthoexciton down-conversion[2]. The rise time of 10 ns is longer than the reported orthoexciton-paraexciton conversion time of 4 ns,[2] presumably because the paraexcitons must also cool down before they appear in the single-photon luminescence, which involves only states near the band bottom.

Another strong evidence is the power dependence of time-resolved data for both paraexcitons and orthoexcitons under the two-photon excitation resonant with the paraexciton state. Fig. 5 shows two important things. First, paraexcitons appear right after the laser pulse, but orthoexcitons are created slowly after a few nanoseconds. Second, orthoexcitons are created more slowly at lower IR laser power, which again indicates a density-dependent process for the creation of orthoexcitons.

All the above results lead us to a model in which paraexcitons are created directly by IR laser pulses resonant with the paraexciton state, then paraexcitons convert to orthoexcitons through a density-dependent process which may be the well-known excitonic Auger process[2,4,14]. In each Auger process, two excitons collide and end up with one exciton recombining and the other exciton ionizing. Because the orthoexciton is a triplet state and the paraexciton is a singlet state, and spin is randomly selected in ionization, 75 percent of the ionized excitons in the Auger process will be returned as orthoexcitons and 25 percent of these excitons will be returned as paraexcitons. This implies that at high excitation power, the density of orthoexcitons will exceed that of paraexcitons after a few nanoseconds, consistent with the results in Fig. 5. The observation that the creation of orthoexcitons becomes slower at lower exciton density is consistent with the fact that the density-dependent Auger process is slower at lower exciton density.

C. Selection rules and polarization dependence in two-photon excitations

The laser pulses we used for the two-photon excitation have spectral width of around 20 nm. One would therefore expect that if the orthoexciton and paraexciton cross sections for two-photon absorption are comparable, that we should then see a significant direct creation of orthoexcitons in addition to paraexcitons, even when the laser is tuned to the paraexciton resonance. The results discussed above indicate that primarily only paraexcitons are being created, however. Is this consistent with the selection rules? Here we take a close look at selection rules of paraexcitons and orthoexcitons in two-photon excitation.

For our one-beam two-photon excitation, the two input beams have the same energy, $\omega_1 = \omega_2 = \omega$, and the same polarization, $\lambda_1 = \lambda_2 = \lambda$. Therefore, the absorption coefficient

in the dipole transition is proportional to:

$$\sum_j |\sum_i \frac{\langle \Gamma_{ex} \mid D_j \mid i\rangle\langle i \mid D_j \mid \Gamma_1^+\rangle}{E_i - \hbar\omega}|^2, \tag{1}$$

where $\mid i\rangle$ are the intermediate states, Γ_1^+ and Γ_{ex} are the vacuum state and the 1s-"yellow" exciton state respectively. $D_j = \hat{\lambda} \cdot p_j$ are possible dipole operators for a certain input polarization λ, where p_j are operators $\hat{x}$, $\hat{y}$ and $\hat{z}$ in three dimensions.

Because the dipole operator is Γ_5^- in the D_{4h} group[15] for the stressed Cu_2O, all allowed internal states should have the negative parity, which could be the p-states in the "yellow" exciton series, the "blue" and "indigo" exciton series[15]. By taking into account the energy difference between the "yellow", "blue" and "indigo" excitons, the dominant internal states are the $2p$-"yellow" excitons with Γ_1^-, Γ_2^-, Γ_3^-, Γ_4^- and Γ_5^- symmetries.

D_{4h} Group	Symmetry	Basis
$2p$-"yellow" excitons	${}^1\Gamma_1^-$	$(x^2-y^2)xyz$
	${}^1\Gamma_2^-$	z
	$2({}^1\Gamma_3^-)$	xyz
	$2({}^1\Gamma_4^-)$	$(x^2-y^2)z$
	$3({}^2\Gamma_5^-)$	x, y
$2s$-"yellow" excitons	${}^2\Gamma_5^+$	yz, zx
	${}^1\Gamma_4^+$	xy
	${}^1\Gamma_3^+$	(x^2-y^2)

TABLE I: The symmetry properties of the intermediate states for both the electric dipole and quadrupole operators in TPE under the stress along the [001] axis[15,16].

To get a general polarization dependence for excitons in the dipole transition, we substitute the three possible dipole operators and possible symmetries of the $2p$-"yellow" exciton states into Equation (1). The calculation result, the polarization dependence for the para and ortho in the dipole transition matrix element under stress along the [001] axis, is explicitly listed in Table 2.

In the quadrupole transition, the absorption coefficient can be calculated in the same way, which is proportional to:

$$\sum_j |\sum_i \frac{\langle \Gamma_{ex} \mid Q_j \mid i\rangle\langle i \mid Q_j \mid \Gamma_1^+\rangle}{E_i - \hbar\omega}|^2, \tag{2}$$

where $\mid i\rangle$ are the intermediate states, Γ_1^+ and Γ_{ex} are the vacuum state and the 1s-"yellow" exciton state respectively. Q_j are possible quadrupole operators for a certain input polarization λ, which are expressed as the following[16]:

$$\begin{aligned} Q &= \sum_{i,j} k_i \lambda_j r_i r_j \\ \Rightarrow Q &= k_x\lambda_x x^2 + k_x\lambda_y(xy) + k_x\lambda_z(xz) + k_y\lambda_x(yx) + \\ &\quad + k_y\lambda_y y^2 + k_y\lambda_z(yz) + k_z\lambda_x(zx) + \\ &\quad + k_z\lambda_y(zy) + k_z\lambda_z z^2 \end{aligned} \tag{3}$$

where $\mathbf{k}$ and λ are wave vector and polarization vector of the input IR beam.

It is not possible to have a mixed dipole-quadrupole transition because the two operators have different parities, and there is no allowed internal state for the mixed transition.

There are five possible quadrupole operators in the D_{4h} group, ${}^2\Gamma_5^+$, ${}^1\Gamma_1^+$, ${}^1\Gamma_3^+$ and ${}^1\Gamma_4^+$, as listed in Table 1. Because the five quadrupole operators have positive parity, all neighboring exciton states with positive parity can be the intermediate states for the two-photon quadrupole transition. However, the dominant internal states are the $2s$-"yellow" exciton states, which are the closest neighbor for paraexcitons and orthoexcitons in energy. The polarization dependence of orthoexcitons and paraexcitons are calculated from Equation (2) with the five possible quadrupole operators and four $2s$-"yellow" exciton states, as listed in Table 2.

According to Table 2, when there is no external stress, the two-photon transition is only allowed for orthoexcitons with polarization dependence of $\sin^2 2\theta + \cos^4\theta$ in the dipole transition, which is confirmed by experimental reports from Kono *et al.*[6] and Kubouchi *et al.*[7]

From the same table, for our [110] laser incident direction, if the stressed crystal is in the D_{4h} group, paraexcitons should be forbidden in both dipole and quadrupole two-photon transitions, which is consistent with the prediction of Inoue-Toyozawa[17], Bader-Gold[18] and Ablova-Bobrysheva[19]. θ is the angle between the polarization of the input laser beam and the horizontal polarization. However, our experimental results in Figure 6 show that there is strong paraexciton luminescence, and the luminescence from both paraexcitons and orthoexcitons has the same intensity for the vertical and horizontal polarizations. This can be explained due to the reduction of the symmetry. That is to say, the crystal is in the D_{2h} group for most of the harmonic potential well, although the crystal is in the D_{4h} symmetry

Symmetry group	Transition	Wave vector **k**	Orthoexciton	Paraexciton
O_h	Dipole	(1, 0, 0)	$\sin^2 2\theta$	Forbidden
		(1, 1, 0)	$\sin^2 2\theta + \cos^4\theta$	Forbidden
		(1, 1, 1)	1	Forbidden
O_h	Quadrupole	(1, 0, 0)	$\sin^2 2\theta$	Forbidden
		(1, 1, 0)	$(1 + a\cos 2\theta)\sin^2\theta$	Forbidden
		(1, 1, 1)	$(1 + a\cos 2\theta + b\cos 4\theta)$	Forbidden
D_{4h}	Dipole	(1, 0, 0)	$\sin^2 2\theta$	$\cos^4\theta$
		(1, 1, 0)	$\sin^2 2\theta + \cos^4\theta$	Forbidden
		(1, 1, 1)	1	$\sin^2 2\theta$
D_{4h}	Quadrupole	(1, 0, 0)	$\sin^2 2\theta$	$\sin^4\theta$
		(1, 1, 0)	$(1 + a\cos 2\theta)\sin^2\theta$	Forbidden
		(1, 1, 1)	$(1 + a\cos 2\theta + b\cos 4\theta)$	$\sin^2 2\theta$
D_{2h}	Dipole	(1, 0, 0)	$\sin^2 2\theta$	$(a\cos^2\theta + b\sin^2\theta)^2$
		(1, 1, 0)	$\sin^2 2\theta + \cos^4\theta$	$(a\cos^2\theta + b\sin^2\theta)^2$
		(1, 1, 1)	1	$(1 + a\cos 2\theta + b\sin 2\theta)^2$

TABLE II: Polarization dependence of orthoexcitons and paraexcitons in the dipole and quadrupole transitions for various symmetries in two-photon excitation, where a and b are constant factors which depend on the matrix elements to the internal states. θ is the angle between the horizontal polarization and the polarization of the input IR beam.

group along the axis of the stress. In the D_{2h} group, the polarization dependence of excitons in the direct dipole transition calculated from Equation 1 is listed in Table 2. For our [110] laser incident direction in the D_{2h} group, the paraexciton follows a polarization dependence of $(a\cos^2\theta + b\sin^2\theta)^2$, where a and b are constant factors. Therefore, if $a = b$, there is no detectable difference between the vertical and horizontal polarization. Because the circular polarization is just a combination of both the vertical and horizontal polarization, we don't expect to see any difference in the exciton photoluminescence intensity when the input laser is changed to the circular polarization from either vertical or horizontal polarization, which is well confirmed by the experimental results in Figure 6.

The orthoexcitons following the exact polarization dependence of the paraexcitons is an-

other good evidence for our proposed model in the resonant two-photon excitation: paraexcitons are created directly by the IR laser and orthoexcitons are created indirectly through a up-conversion of the paraexcitons.

Moreover, we also note that the birefringence changes the polarization of the incident infrared laser beam and the changes are different at different positions in the harmonic potential well. In general, there is substantial polarization mixing for the whole harmonic trap.

At this point, one may ask why the paraexciton dipole and quadrupole matrix elements should dominate the creation of excitons in our two-photon excitation, since the orthoexciton transitions are allowed. One reason is that the IR laser is tuned to the resonant wavelength of the paraexciton state in this work, which gives an on-resonant two-photon excitation for paraexcitons and an off-resonant three-photon excitation for orthoexcitons. Moreover, all our experiments except Figure 6 are done with a vertically polarized IR laser, that is to say, $\theta = 90^0$ in Table 2, which means that the orthoexciton polarization dependence for our [110] laser incident direction in the D_{2h} group is $\cos^4\theta + \sin^2 2\theta = \cos^4(90^0) + \sin^2(180^0) = 0$. Therefore, the orthoexciton dipole matrix element is forbidden for most of this work. At $\theta = 0^0$, the horizontal polarization, we would expect some orthoexcitons created directly by the IR laser, but the matrix element may be smaller.

Therefore, we can explicitly express our results as the following: confined by a harmonic potential trap created with an external stress, when an IR laser pulse tuned to one half the paraexciton ground-state energy is shining along the [110] crystalline direction of the Cu_2O sample, paraexcitons are directly created by the IR laser pulse, and orthoexcitons are created primarily from the paraexciton up-conversation process at the early time after the laser pulse.

D. Is there BEC of paraexcitons?

Since we can resonantly create the paraexciton via resonant two-photon excitation, should we see BEC of the paraexcitons? Our estimate of the density of paraexcitons indicates that we should not expect to see this. Fig. 7 shows an integrated spatial profile of the paraexciton in the Cu_2O crystal at 1.6 Kelvin, which gives the paraexciton excitation volume $V = \frac{4}{3}\pi(20\mu m)^3$. As mentioned in Section (3.B), when detected by PMT, the 250 KHz resonant

IR laser with average power of 70 mW creates the same exciton luminescence intensity via two-photon excitation as the 3.8 MHz dye-laser at 607.5 nm with 0.9 mW average power does via single-photon excitation. If we assume that 5% of the 0.9 mW average power is absorbed in the single-photon excitation[20], that one absorbed photon creates one exciton in the single-photon excitation, and that comparable luminescence intensity implies comparable exciton density, then we find the density of excitons in the two-photon excitation is

$$n = \frac{3.8MHz}{250KHz} * \frac{0.9mW * 5\%}{3.8MHz * \frac{2\pi\hbar c}{\lambda} * V} = 1.6 * 10^{16} cm^{-3}. \quad (4)$$

where c is the speed of light, $\frac{2\pi\hbar c}{\lambda}$ is a single photon energy in the single-photon excitation with a laser at 607.5 nm, and the ratio $\frac{3.8MHz}{250KHz}$ is the calibration of the photon-counting efficiencies in the time-correlated single photon detection for the two laser systems with different repetition rates. This corresponds to 0.06% absorption of the infrared laser light.

To calculate the critical exciton density for BEC, we have to know the exciton temperature, which can be calculated in two ways. One way is to fit high temperature tail of the paraexciton luminescence with a Bose distribution function, $\varepsilon^{1/2}/(e^{\varepsilon/(k_B T)} - 1)$, where ε is paraexciton energy. The other way is to find the full width at half maximum of the phonon-assisted luminescence line, which is equal to $3.4k_B T$ in a three-dimensional harmonic potential trap[2]. Our calculations from the above two ways indicate that the exciton has a minimum temperature of 7 Kelvin, which means the critical exciton density should be $5 * 10^{17} cm^{-3}$.[1] Since the created paraexciton density is about thirty times less than the required density for BEC, we do not expect to establish BEC of paraexcitons even with the maximum laser power from our laser system. With higher laser power or lower temperature, however, the paraexciton critical density can be approached with resonant two-photon excitation which creates paraexcitons directly.

In order to know whether the density-dependent Auger process is the only paraexciton up-conversion process, we can do an interesting comparison between Figure 5 and our former work[2,14]. The former work gives the Auger constant of $3 * 10^{-17}\mathrm{cm}^3/\mathrm{ns}$ around 1.9 kbar, which implies a decay rate of 2 ns and 4 ns for the input IR laser power of 90 mW and 45 mW, respectively. While Figure 5 gives different decay rates, 3 ns for the 90 mW laser and 10 ns for the 45 mW. There are several reasons for the big inconsistency. First, there may be other up-conversion processes for the paraexciton besides the density-dependent Auger process. Moreover, the paraexcitons must also cool down before they appear in the

single-photon luminescence.

IV. CREATING EXCITONS WITH TWO COLLIDING PULSES

Besides doing experiments with one-beam, two-photon excitation resonant with the paraexciton state, we can excite excitons with two colliding pulses, that is to say, split the IR laser beam into two parts and shine them into the Cu_2O sample, such that both pulses reach the exciton stress trap at the same time. In this case, the $\vec{k} = 0$ state is directly excited if the two parts travel in opposite directions. Therefore, the created excitons have zero momentum, $\vec{k} = 0$, which means the ground state is directly excited, where the condensate should appear, if one photon is from each pulse.

The experimental set-up is shown in Fig. 1. In order to make the two beams meet at the same time in the Cu_2O sample, we added a two-mirror delay system controlled by a precise translation stage. Fig. 8 shows the dependence of the exciton luminescence intensity on the time delay between the two colliding pulses. A comparison between one-beam and two-beam resonant excitations with the same total laser power, 90 mW, is shown in Fig. 9. The exciton luminescence in the one-beam excitation is brighter than that of the two-beam excitation, and creation of orthoexcitons in the one-beam excitation is faster than with the two-beam excitation, which indicates more excitons are created in the one-beam excitation.

To explain this phenomenon, one must consider the dependence of the density of states on the momentum $\vec{k}$. In the case of two photons travelling in the same direction, the excitons are created in the region of the (weak) polariton mixing. Two photons travelling in opposite directions will create an exciton at $\vec{k} = 0$, where the density of states is much lower. In the case of two-beam excitation, there will also be one-beam excitation with half of the total power of the two-beam excitation. Since the exciton density in the two-photon process is proportional to the square of laser power, the one-beam excitation with half of the total power will have one fourth the efficiency. The sum of all processes in the two-beam excitation ends up being less than the total in the one-beam case.

V. CONCLUSION

We resonantly create paraexcitons with an IR laser beam tuned to one half the paraexciton ground-state energy. This is surprising, since it is generally assumed that the cross section for paraexciton creation is always much less than that for orthoexciton. Our experimental results are all consistent with this result, however, including the polarization dependence and time-dependent data. The exciton creation efficiency in resonant two-photon excitation is greater for one-beam excitation than for two colliding pulses, but the colliding pulse method may be useful for direct creation of a condensate in the ground state. At present, the paraexciton density in this work is thirty times less than the required density for BEC of paraexcitons, but with higher laser power from stronger IR laser sources or lower temperature, the critical density can be approached with one-beam two-photon excitation resonant with the paraexciton state.

Acknowledgements. This work has been supported by CRDF-MRDA Award No. MP2-3026 and NSF Award No. DMR-0102457. Samples of Cu_2O were obtained from P. J. Dunn of the Smithsonian Institute. We would like to thank Robert P. Devaty for discussions on group theory, Albert Heberle for suggestions on spectral filtering, M. Kuwata-Gonokami of Tokoyo university on the selection rules and thank Vincenzo Savona for helpful conversations on the two-beam, two-photon excitation.

---

[1] S. A. Moskalenko and D. W. Snoke, *Bose-Einstein Condensation of Excitons and Biexcitons*, (Cambridge University Press, 2000).

[2] S. Denev and D. W. Snoke, Phys. Rev. B **65**, 085211 (2001).

[3] V. C. Negoita, Ph.D. thesis, University of Pittsburgh, (2001).

[4] D. W. Snoke and V. Negoita, Phys. Rev. B **61**, 2904 (2000).

[5] N. Naka and N. Nagasawa, Phys. Rev. B **65**, 075209 (2002).

[6] S. Kono, M. Hasuo, and N. Nagasawa, J. Lumin. **66/67**, 433 (1996).

[7] M. Kubouchi, K. Yoshiot, R. Shimano, A. Mysyrovwicz and M. Kuwata-Gonokami, APS/123-QED, in press (2004).

[8] A. Jolk, M. Jorger, and C. Klingshirn, Phys. Rev. B **65**, 245209 (2002).

[9] Y. Sun, G. K. L. Wong and J. B. Ketterson, Phys. Rev. B **63**, 125323-1 (2001).

[10] M. Y. Shen et al., Phys. Rev. B **53**, 13477 (1996).

[11] N. Naka and N. Nagasawa, Solid State Comm. **110**, 153 (1999).

[12] N. Naka and N. Nagasawa, Proceedings of the 26th ICPS, Edingburgh (2002).

[13] D. P. Trauernicht, J. P. Wolfe, and A. Mysyrowicz, Phys. Rev. B **34**, 2561 (1986).

[14] Yingmei Liu and David Snoke, "Temperature dependence of exciton Auger decay process in Cu_2O", cond-mat/0408184 (2004).

[15] G. F. Koster, J. O. Dimmock, R. G. Wheeler, and H. Statz, "Properties of the Thirty-two Point Groups", (MIT Press, Cambridge, Mass, 1963)

[16] Yingmei Liu, Ph.D. thesis, University of Pittsburgh, (2004).

[17] M. Inoue and Y. Toyozawa, J. Phys. Soc. Japan **20**, 363 (1965).

[18] Todd R. Bader and Albert Gold, Phys. Rev. **171**, 997 (1968).

[19] L. A. Ablova and A. I. Bobrysheva, Sov. Phys. Semicond., Vol. 7, No. 6, 712 (1973).

[20] D. W. Snoke and V. Negoita, Phys. Rev. B **61**, 2904 (2000).

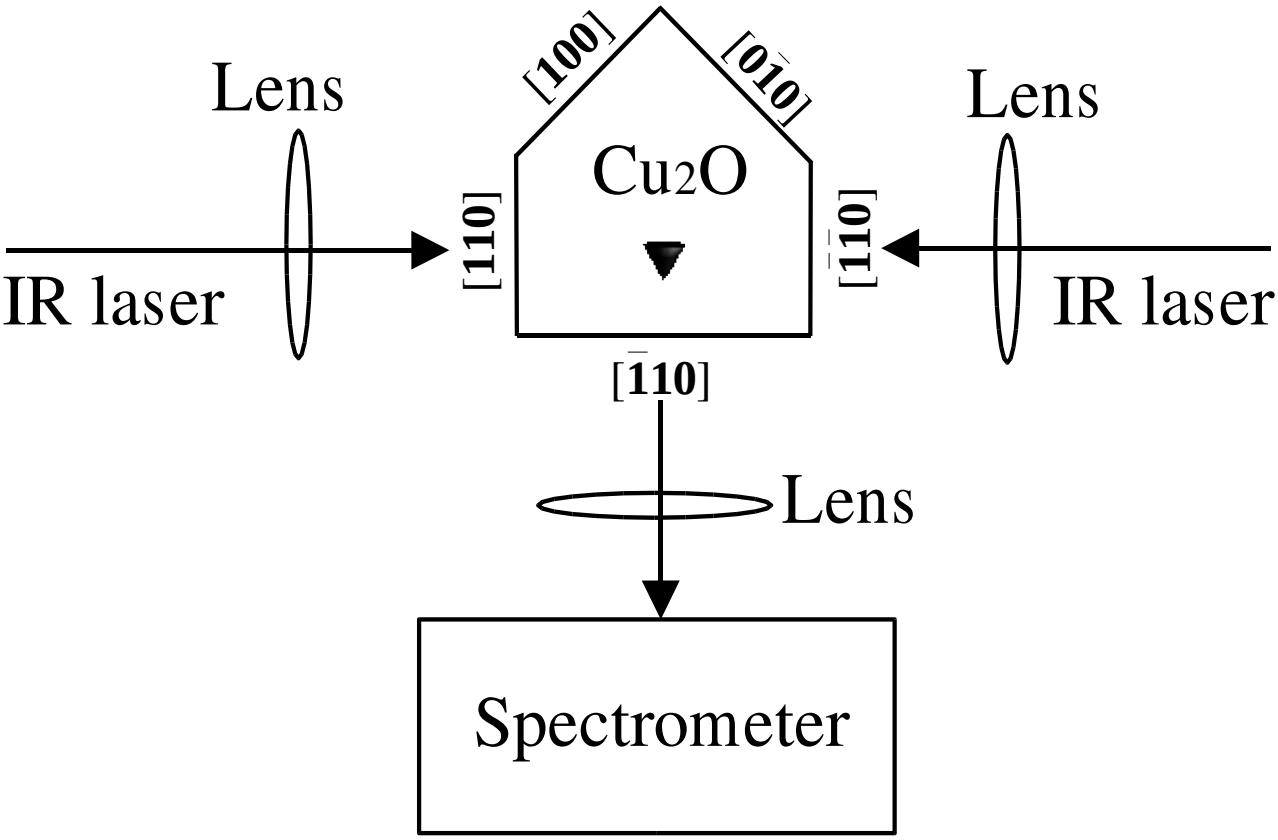


FIG. 1: Schematic of the experimental set-up in this work.

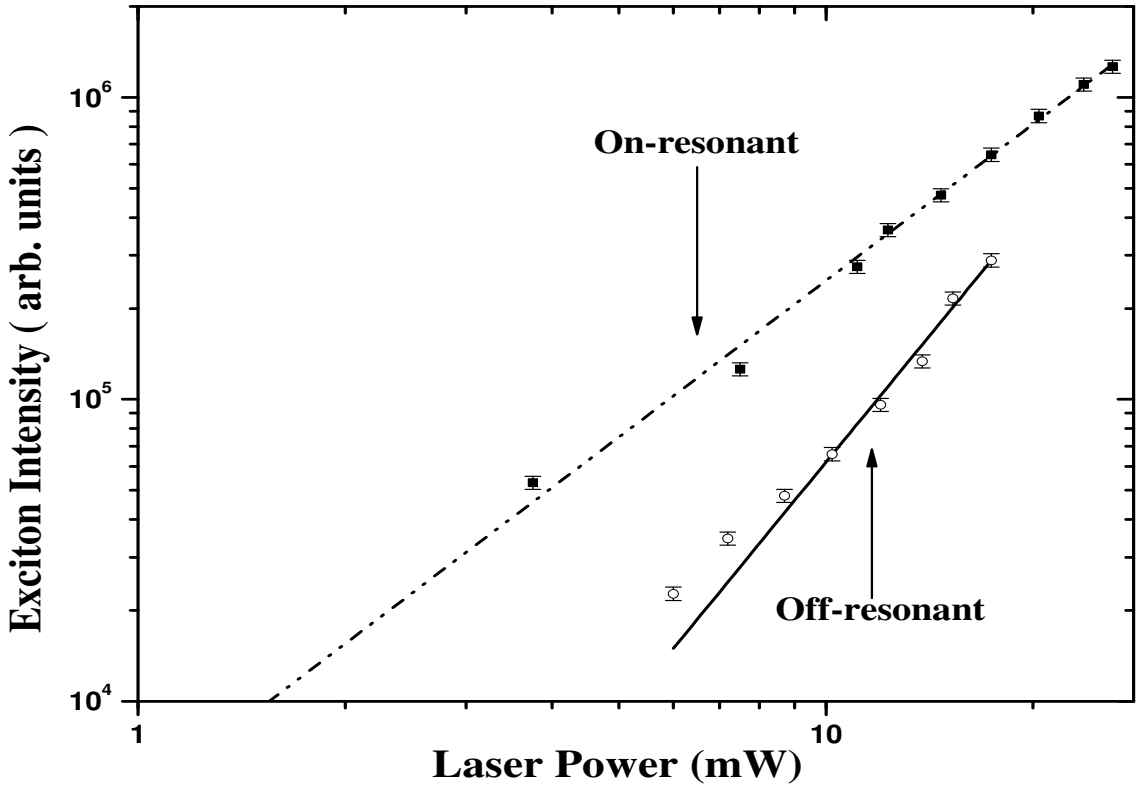


FIG. 2: When the IR laser is at 1228 nm, resonant with the paraexciton state, integrated exciton luminescence intensity (black squares in the figure) can be best fit to $P^{1.7\pm0.1}$ (black dashed line), where P is the input laser power. This is consistent with a two-photon process within the experimental error. If the laser is off-resonant, at 1240 nm, the integrated exciton luminescence intensity (black open circles) can be best fit to $P^{2.8\pm0.2}$ (black solid line in the figure), consistent with a three-photon process.

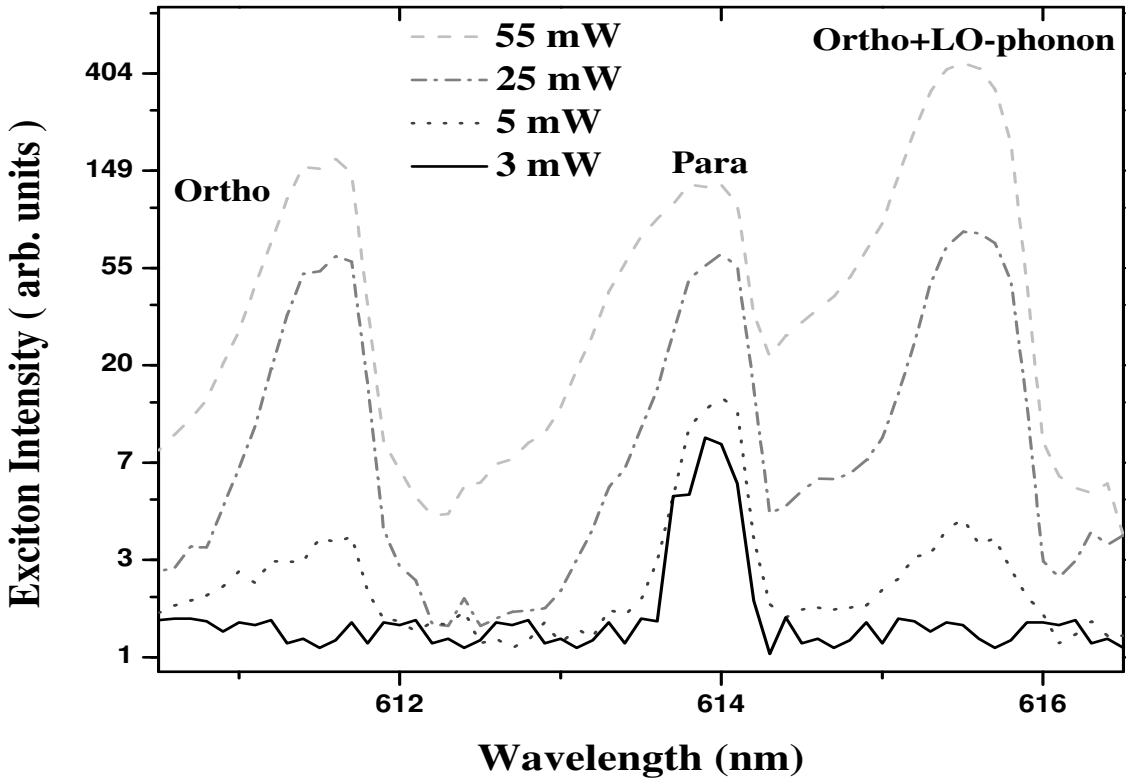


FIG. 3: Time-integrated exciton luminescence intensity in the Cu_2O sample for several different laser powers, at 1.6 Kelvin and under 1.9 kbar stress along the [001] direction, with two-photon one-beam excitation resonant with the paraexciton state.

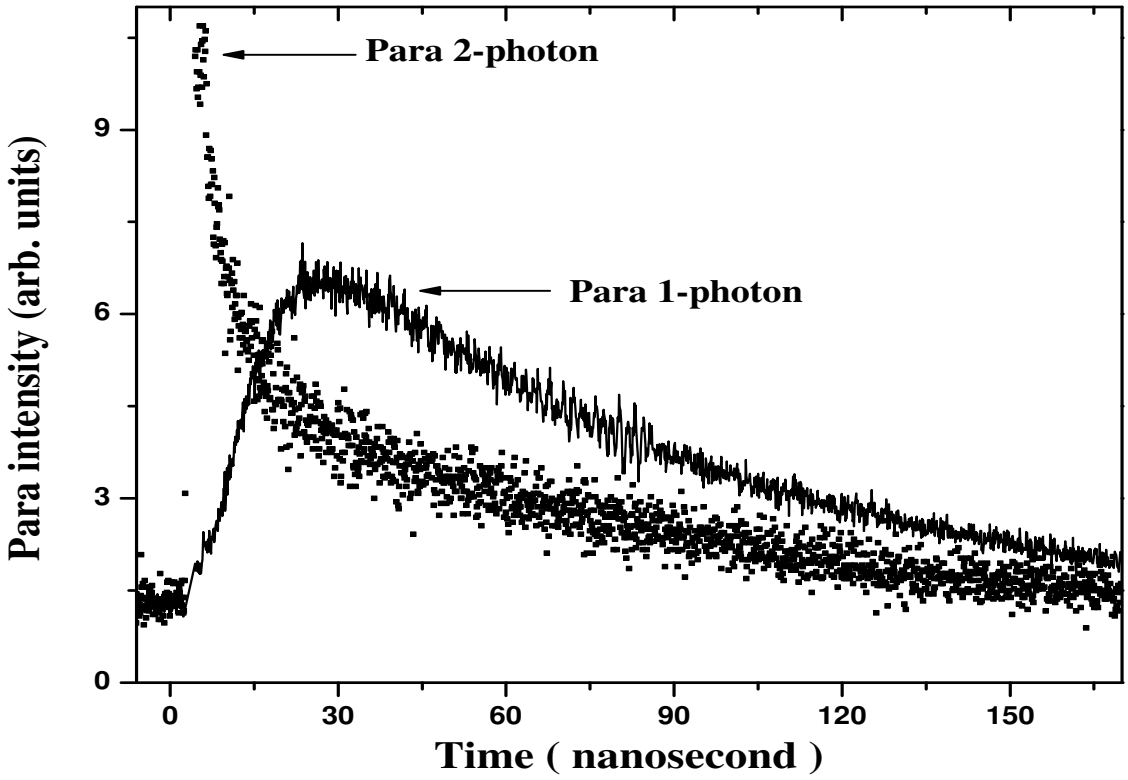


FIG. 4: Paraexciton luminescence as a function of the time after the laser pulse, for a Cu_2O sample at 1.6 Kelvin and under 1.9 kbar stress along the [001] direction. Black dots: two-photon excitation resonant with the paraexciton state. Black solid line: single-photon excitation tuned to the bottom of the orthoexciton phonon-assisted absorption. The power of the red and the IR laser were adjusted to give the same total integrated exciton luminescence intensity.

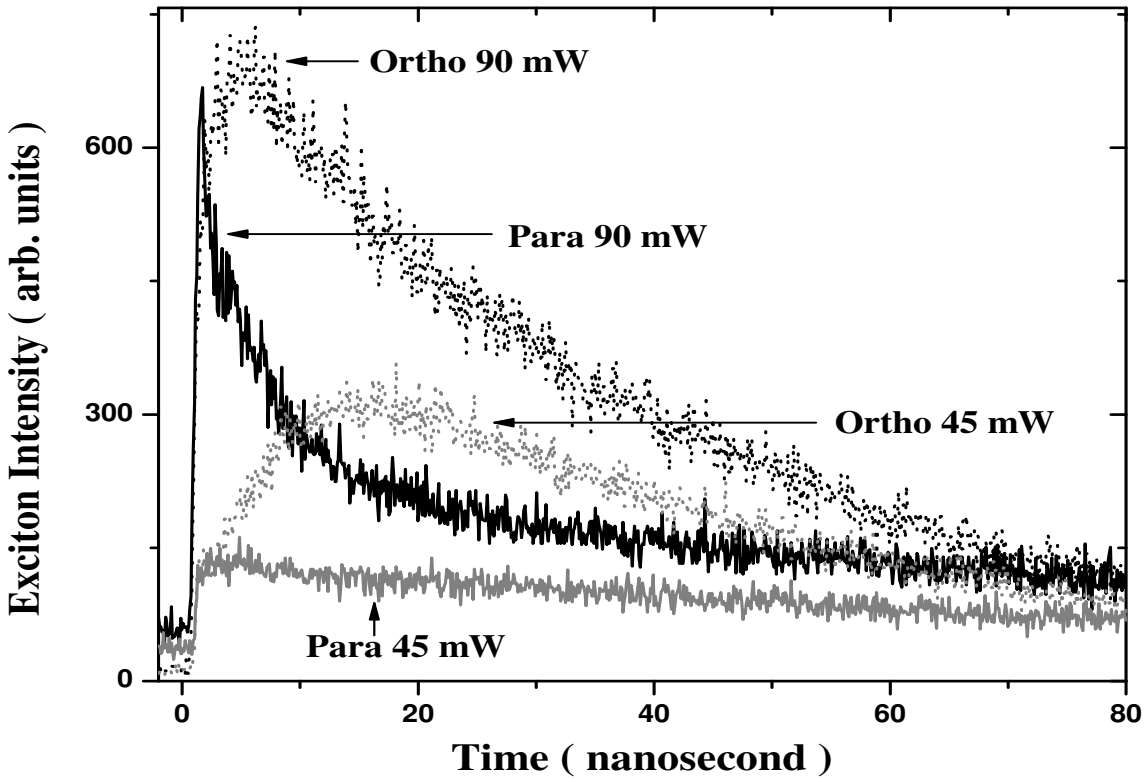


FIG. 5: Time-resolved paraexciton and orthoexciton luminescence in the Cu_2O sample for two different laser powers, at 1.6 Kelvin and under 1.9 kbar stress along the [001] axis, with two-photon excitation resonant with the paraexciton state. The black dots and black solid line are the orthoexciton and paraexciton luminescence intensity at laser power of 90 mW, respectively, and the gray dots and gray solid line are the orthoexciton and paraexciton luminescence intensity at laser power of 45 mW, respectively.

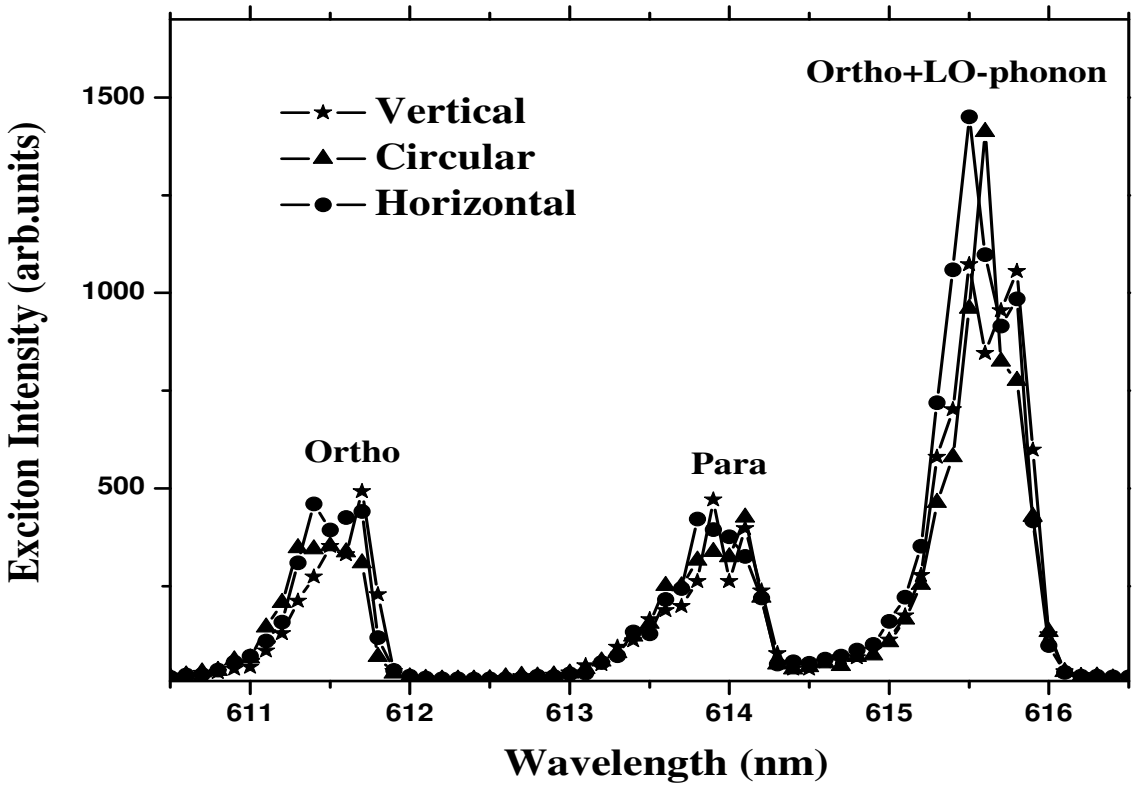


FIG. 6: Polarization dependence for the total integrated paraexciton and orthoexciton luminescence intensities for a Cu_2O sample at 1.6 Kelvin under 1.9 kbar stress along the [001] direction, with two-photon excitation resonant with the paraexciton state.

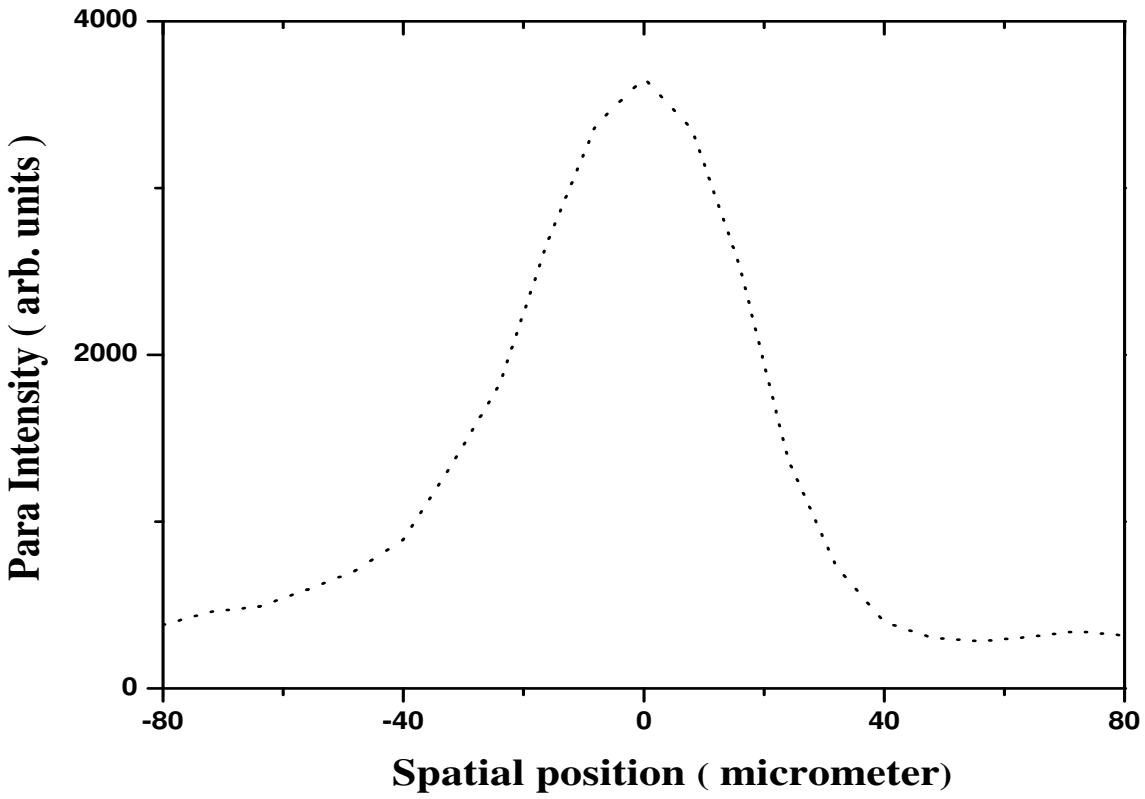


FIG. 7: Spatial profile of the paraexciton luminescence in the stress-induced harmonic potenial trap for the excitons, for the Cu_2O sample at 1.6 Kelvin under 1.9 kbar stress along the [001] direction, with two-photon excitations resonant with the paraexciton state.

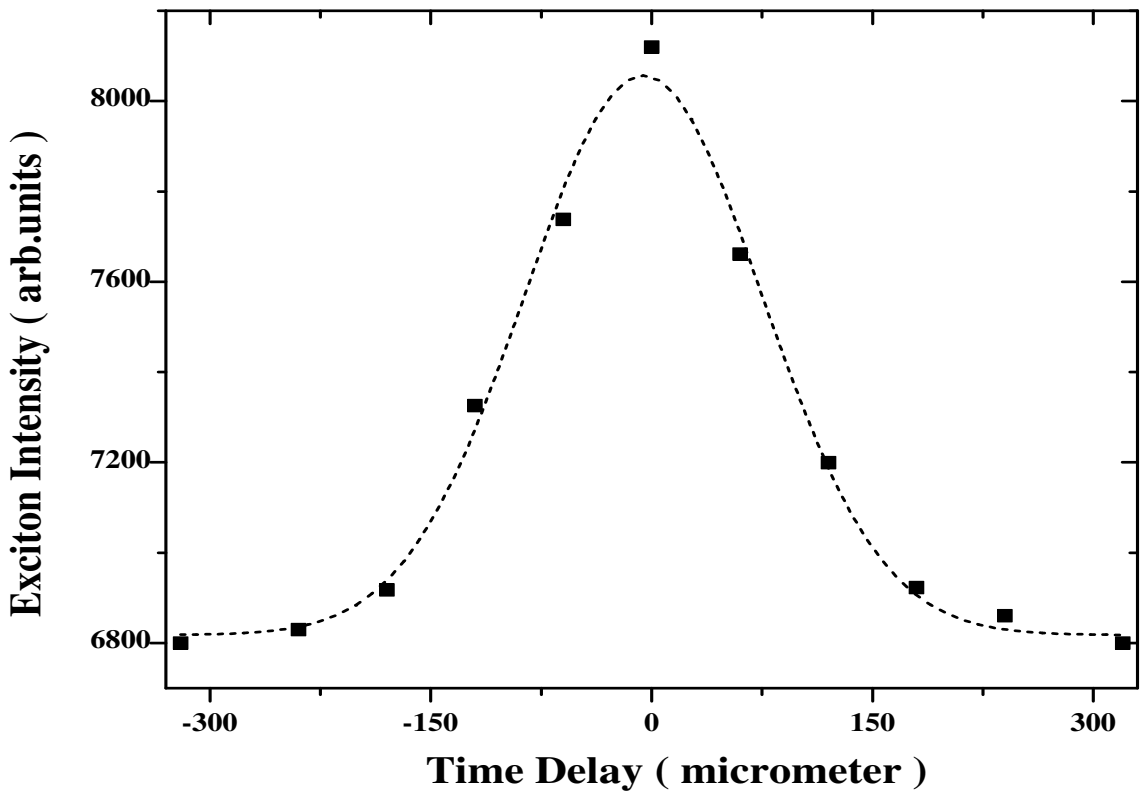


FIG. 8: Total integrated exciton luminescence intensity as a function of the time delay between two laser pulses for two-beam, two-photon excitation resonant with the paraexciton state, for the Cu_2O sample at 1.6 Kelvin under 1.9 kbar stress along the [001] direction. Black squares: experimental data. Dashed line: Gaussian fit.

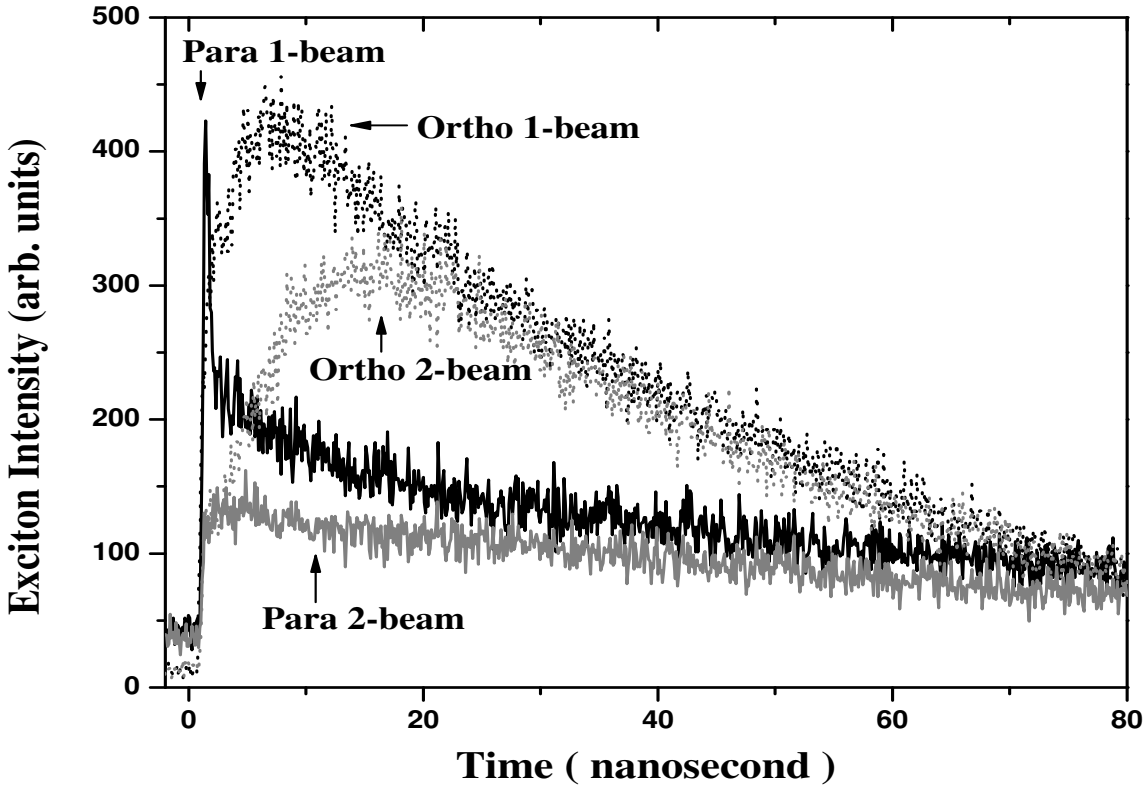


FIG. 9: Exciton luminescence intensity as a function of the time after the laser pulses for one-beam and two-beam two-photon excitation resonant with the paraexciton state, with the same total laser power, for the Cu_2O sample at 1.6 Kelvin under 1.9 kbar stress along the [001] direction. The black dots and and the black solid line are orthoexciton and paraexciton luminescence intensity, respectively, for one-beam excitation, and the gray dots and gray solid line are the orthoexciton and paraexciton luminescence intensity, respectively, for the two-beam excitation.